Journal of Alloys and Compounds 509 (2011) 8607–8613

Contents lists available at ScienceDirect

Journal of Alloys and Compounds

journal homepage: www.elsevier.com/locate/jallcom

Effects of ultrasonic treatment on the tensile properties and microstructure of twin roll casting Mg–3%Al–1%Zn–0.8%Ce–0.3%Mn (wt%) alloy strips

Jun Zhao [a], Kun Yu [a,*], Xinying Xue [a], Daheng Mao [b], Jianping Li [b]

[a] School of Materials Science and Engineering, Central South University, Changsha 410083, China
[b] College of Mechanical and Electrical Engineering, Central South University, Changsha 410083, China

HIGHLIGHTS

- Ultrasonic treatment promoted grain refinement of α-Mg and modification of intermetallic $Mg_{17}(Al,Zn)_{12}$ and MgAlCeMn phases.
- Both the yield strength and elongation of twin roll casting Mg alloy strip improve obviously with ultrasonic treatment.
- The grain multiplication and the cavitation-induced heterogeneous nucleation by ultrasonic treatment lead to the refinement of Mg alloy grains.
- The undercooling created by the cavitation of ultrasonic treatment cause the morphology modification of second phases.

ARTICLE INFO

Article history:
Received 22 May 2011
Accepted 14 June 2011
Available online 21 June 2011

Keywords:
Metals and alloys
Magnesium alloy
Mechanical properties
Microstructure
Twin roll casting
Ultrasonic treatment

ABSTRACT

Twin roll casted Mg–3%Al–1%Zn–0.8%Ce–0.3%Mn alloy strips with thicknesses of approximately 3.6–4 mm are prepared, and the effects of ultrasonic treatment on their tensile properties and microstructure are investigated. The results show that, after treatment with an ultrasonic power of 800 W, the grain size of α-Mg decreased from 136.3 μm to 44.7 μm, and the morphology changed from dendritic to globular. Grain multiplication by fragmentation of dendrites and cavitation-induced heterogeneous nucleation are the mechanisms of refinement of the α-Mg grains by ultrasonic treatment. The needle-like shaped intermetallic MgAlCeMn is modified by ultrasonic treatment and obtains a more globular shape with finer particles. This change was a result of undercooling created by the cavitation of ultrasonic treatment. This improved microstructure contributes to an increase in both tensile strength and elongation of twin roll casting magnesium alloy. The yield strength of the experimental alloy strips subjected to 800 W ultrasonic treatment is approximate 30% higher than that of alloy without ultrasonic treatment. Furthermore, the elongation of experimental alloy is almost double that of alloy without ultrasonic treatment. The relationship between the yield strength and the refined grain size of the experimental alloy can be expressed by the Hall–Petch equation $\sigma_y = 74.8 + 31.4 \times d^{-1/2}$.

1. Introduction

Magnesium alloys are the lightest structural alloys for commercial applications, and they have recently been the subject of increased research and development efforts [1]. Magnesium alloy sheet products are needed for numerous weight-sensitive applications, such as automotive body components [2]. However, it is difficult to fabricate magnesium alloy sheets by conventional processes, which involve hot-rolling slabs by direct chill (DC) casting. These manufacturing difficulties are primarily the result of the poor workability and deformability of magnesium alloys, which require frequent intervening reheating procedures during hot rolling [3,4]. As a result, magnesium alloy sheets from DC casting ingots are more expensive than steel and aluminum alloys. The higher price of magnesium alloy sheets has prevented their widespread application in automobile manufacturing [5]. One of the keys to solving this problem is the twin roll casting (TRC) process, which is capable of manufacturing magnesium alloy strips with a thickness less than 10 mm (conventional ingot methods produce thicknesses of approximately 200–300 mm) [6]. Compared to the DC casting processes, the primary advantage of continuous TRC technology is that it eliminates several of the steps in the manufacture of the final sheet products [7].

As discussed in a previous publication [8], the alloys fabricated by TRC always have narrow freezing ranges that prevent the centerline segregation by the separation force in the two phase region (solid + liquid) during solidification. Therefore, the alloy AZ31 (Mg–3%Al–1%Zn), which has a relatively narrow equilibrium freezing range ($\Delta T = 66$ K), is a good candidate for TRC magnesium alloy strip manufacturing [9]. An alternative approach is the

* Corresponding author. Tel.: +86 731 88879341; fax: +86 731 88876692.
E-mail address: yukungroup@gmail.com (K. Yu).

0925-8388/$ – see front matter © 2011 Elsevier B.V. All rights reserved.
doi:10.1016/j.jallcom.2011.06.060

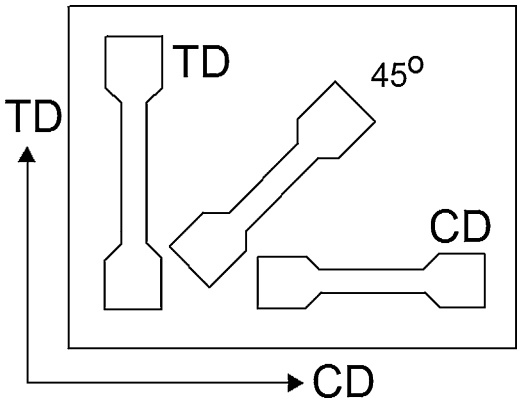

Fig. 1. Schematic diagram of tensile test specimen orientation.

incorporation of alloying elements, which have limited solid solubility, into the magnesium matrix. These additions may produce alloys that are more suitable for TRC due to their faster solidification rate compared to conventional DC casting. The use of manganese in the alloy TRC AZ91 and in an Mg–Zn-based alloy illustrates that such an approach can improve the strength and corrosion resistance of magnesium alloys [10–12]. Furthermore, the addition of cerium to an Mg–Al–Zn alloy results in increased oxidation resistance of the molten magnesium liquid and refinement of the as-cast grains [13]. The Mg–Ce-based alloy also provides high strength and good plastic deformability at ambient and high temperatures [14,15]. Therefore, in this investigation, the Mg–3%Al–1%Zn–0.8%Ce–0.3%Mn alloy (wt%, nominal composition) is designed and prepared by the TRC technology to develop magnesium alloy sheets for evaluation.

It is well known that the major problems with TRC magnesium alloy strips are coarse columnar grains, coarse deleterious intermetallic phases and surface/edge cracks [6,9]. Ultrasonic treatment (UST) is a useful technique to improve aluminum and magnesium alloy casting quality [16,17]. However, there have been no previously published investigations on the effects of UST on magnesium alloy strip fabrication by TRC. In the present investigation, our objective is to develop high-quality TRC magnesium alloy strips by utilizing UST of the molten experimental alloy to improve the quality of the alloy during the TRC process. We have also evaluated the experimental alloy with and without UST to clarify the effects of this treatment on the microstructure and properties of TRC magnesium alloy strips.

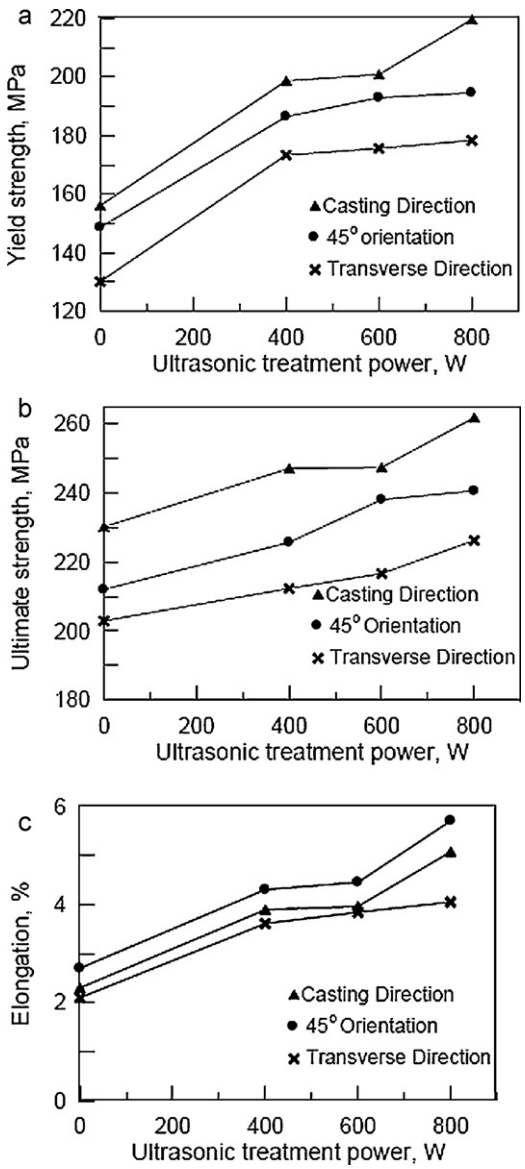

Fig. 2. Effects of different ultrasonic powers on the tensile properties of twin roll casting experimental alloy strips along different directions (a) effects on the yield strength; (b) effects on the ultimate strength and (c) effects on the elongation.

2. Material and methods

The analyzed chemical composition of the experimental alloy used in this study was Mg–2.45%Al–0.92%Zn–0.69%Ce–0.21%Mn (wt%). The alloy was melted at 953 K and transferred into a preheated header box with a temperature over 973 K. The twin roll caster used in this experiment was a lab-scale version of a TRC machine with a pair of opposed steel rollers, which were 400 mm in diameter and 500 mm in width. The rollers featured an inner water-cooled system and had an adjustable rotation speed and roller gap. The contact length between the rollers and the molten metal was 45–46 mm. The roll casting speeds were varied from 2.5 to 2.8 m/min according to the stream of alloy liquid. The width of the TRC experimental alloy strip was set to 260 mm.

Under the protection of a CO_2 + 0.5 vol.% SF_6 gas mixture, the molten experimental alloy was treated with the ultrasonic waves in the header box during TRC. The ultrasonic oscillation device used in this experiment consisted of an acoustic generator and transducer with a horn. The horn was immersed to a depth of approximately 10–15 mm in the molten alloy within the header-box throughout the TRC procedure. It is well known that the efficiency of UST is influenced by the amplitude and frequency of the vibrations [18]. The amplitude of the ultrasonic vibration is directly related to the ultrasonic power. Higher ultrasonic power input results in higher amplitude. Input powers of 400 W, 600 W and 800 W were utilized by the ultrasonic generator to assess their effects on the molten experimental alloy liquid. At the same time, cavitation intensity created by the ultrasonic vibrations in the liquid metal was inversely related to the ultrasonic frequency. Hence, in compromised conditions, UST should be performed using lower frequencies and higher amplitudes. The fixed frequency of the ultrasonic vibrations was 20 kHz ± 200 Hz. The holding time of the UST in the liquid was also important. Because the TRC process ran continuously throughout the experiment, the ultrasonic vibrations in the header box were also continuous. The thickness of the TRC experimental alloy strips produced was between 3.6 and 4 mm.

Tensile test specimens were machined from the TRC Mg–Al–Zn–Ce–Mn alloy strips with or without UST in as-cast conditions. The TRC alloy strips without UST were prepared as control specimens. Three kinds of tensile samples were machined from the TRC strips: parallel to casting direction (CD), transverse to casting direction (TD) and an intermediate (45°) orientation (Fig. 1). Tensile testing was performed on an Instron 8032 mechanical testing machine in accordance with ASTM standard B557M-94.

The observations of the microstructure of the experimental alloy were made using a Polyvar-MET metallographic microscope. Morphology and composition analysis of intermetallics were determined using a JSM-5600Lv scanning electron microscopy (SEM) and energy dispersive X-ray spectroscopy (EDS). The measured metallographic parameters of the experimental alloy samples, such as average grain size and area and perimeter of intermetallics, were calculated using the LEICA metallographic analysis system. The samples for microstructure observation were polished with emery paper and etched in a solution of 0.5 vol.% nitric acid–ethanol.

3. Results

3.1. Tensile properties of experimental Mg–Al–Zn–Ce–Mn alloys

The tensile tests were conducted to determine the effects of UST on the tensile strength and elongation of the specimens and to investigate the connection between mechanical properties and microstructure. Fig. 2 shows the effects of different UST powers on the yield strengths, ultimate strengths and elongations of TRC experimental alloy in the as-cast state in different orientations. For all UST powers, the yield and ultimate strengths of the CD samples were higher than the 45° samples or the TD samples. The highest elongation value was found in the 45° samples, and the elongation values of the CD samples were higher than the TD samples. The varied strength and elongation values obtained for the samples taken using different orientations demonstrated that the TRC experimental alloy strips possessed anisotropic properties. The slight thickness reduction of the as-cast strip (usually approximate 10%) during the TRC process increased the strength along the casting direction. Analysis of the samples taken from different orientations demonstrated that the anisotropic behavior was within acceptable limits.

We also observed that all the mechanical properties increased with an increase in the UST power from 400 W to 800 W. The yield strength of the TRC experimental alloy strip subject to 800 W UST was approximately 30% higher than that of the TRC alloy without UST. The elongation value of the TRC alloy subject to UST was almost double that of the alloy without UST. This improvement was primarily the result of the finer microstructure of the TRC Mg–Al–Zn–Ce–Mn alloy treated with UST.

3.2. Microstructure of experimental Mg–Al–Zn–Ce–Mn alloys

Fig. 3 shows cross sections that reveal the microstructure of TRC experimental alloys with and without different applied UST power levels. The microstructure of TRC experimental alloys without UST showed the typical dendrites of primary α-Mg phase. The dendrites of the TRC experimental strips were coarse, and the calculated average diameter of the grain was 136.3 μm (Fig. 3a). The largest measured diameter of the grain was 188.2 μm, and the finest was 70.6 μm. Such coarse dendrites and heterogeneous grains in the TRC experimental alloy strips were detrimental to the mechanical properties.

However, the UST had important effects on the refinement of the α-Mg phase dendrites. As shown in Fig. 3(b–d), increasing the applied UST power reduced the grain size and changed the morphology of the grains from dendritic structure to spherical shape. Even with a relatively low power of 400 W, the UST significantly changed approximately half of the dendritic primary α-Mg to a spherical shape (Fig. 3b). The measured average diameter of the grains was reduced to 78.3 μm. It was evident that, with increasing UST power, the grain size reduced, and the grains became more uniform. There were few dendrites present in materials treated with a UST power of 600 W (Fig. 3c). The equivalent circle diameter of the dendrites or the grain size dropped to 66.8 μm. Although some grains were still dendritic, they possessed fewer branches and shorter arms, which resulted in smaller grain diameters. With a high UST power of 800 W, all dendritic grains had changed to uniform spherical grains and possessed an average diameter of 44.7 μm (Fig. 3d).

To further understand the effects of UST on the microstructure of the TRC experimental alloys, SEM micrographs were taken, and analysis of intermetallic phases was performed (Fig. 4). The identification of EDS and the analysis of Mg–Al–Zn phase diagram demonstrate that there were two typical intermetallics detected in the microstructure of the TRC Mg–3%Al–1%Zn–0.8%Ce–0.3%Mn alloy (Fig. 4a). The first, the $Mg_{17}(Al,Zn)_{12}$ phase, possessed a relatively spherical shape (Fig. 4b). The second, the MgAlCeMn phase, had a needle-like shape (Fig. 4c). The addition of a minor amount

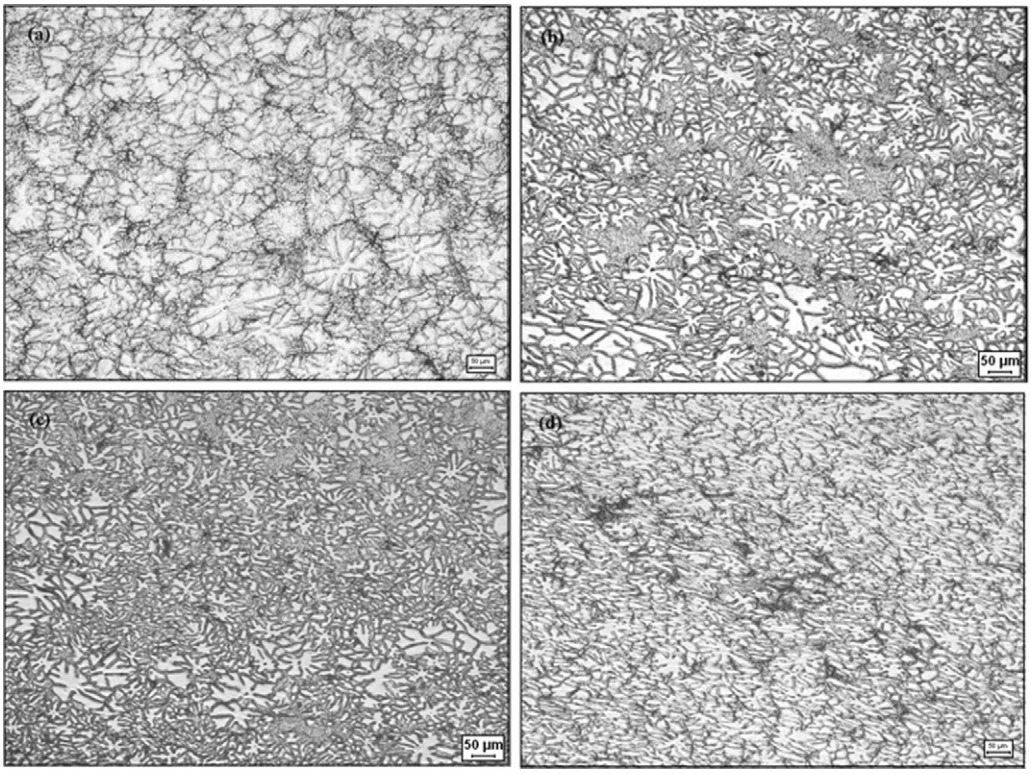

Fig. 3. Microstructures of twin roll casting experimental alloy strips with different ultrasonic treatment powers (a) twin roll casting alloy without ultrasonic treatment; (b) twin roll casting alloy with ultrasonic treatment of 400 W; (c) twin roll casting alloy with ultrasonic treatment of 600 W and (d) twin roll casting alloy with ultrasonic treatment of 800 W.

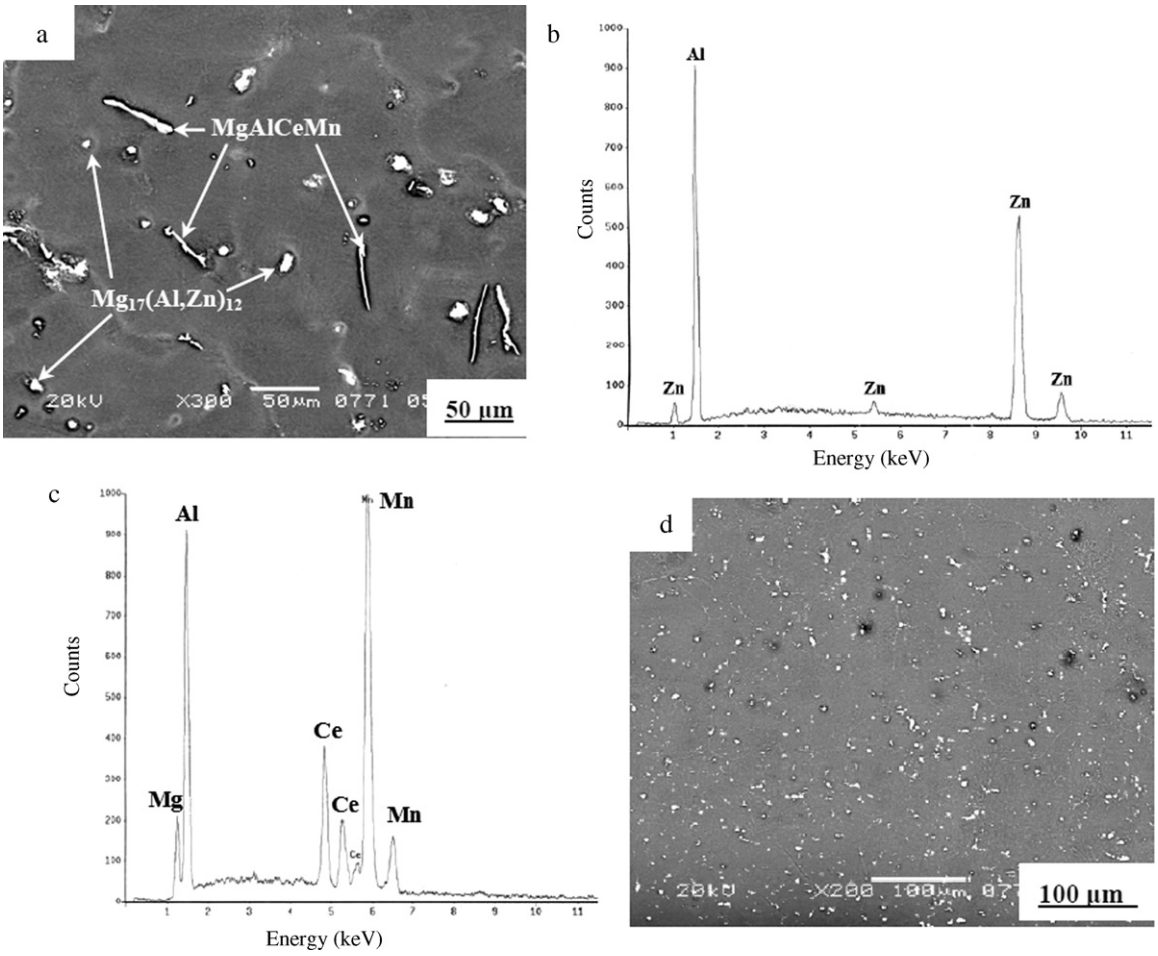

Fig. 4. SEM micrographs and EDS identifications of intermetallics in experimental alloy strips (a) morphology of intermetallics without ultrasonic treatment; (b) composition analysis of the $Mg_{17}(Al,Zn)_{12}$ phase; (c) composition analysis of the MgAlCeMn phase and (d) morphology of intermetallics with ultrasonic treatment of 800 W.

of cerium could improve the oxidation resistance and reduce the flammability of molten magnesium effectively [14]. Such an addition of cerium was helpful in protecting the magnesium alloy liquid during TRC. Furthermore, both cerium and manganese could react with impurities, such as iron, copper or nickel, in the molten Mg–Al–Zn system alloy [12]. Typically, the addition of two such elements is sufficient to ensure removal of impurities from the molten alloy. However, excess cerium and manganese also reacted with magnesium and aluminum to form needle-like intermetallics. Upon application of UST to the TRC Mg–Al–Zn–Ce–Mn alloy, the morphology of the intermetallics, including both the $Mg_{17}(Al,Zn)_{12}$ and the MgAlCeMn phases, was significantly modified in shape and refined in size (Fig. 4d).

The characteristics of intermetallics affected the deformability and quality of the TRC magnesium alloy strips during the casting process. The high hardness and the angular shape of the MgAlCeMn phase caused a great mismatch between the intermetallic and the magnesium matrix, and this mismatch led to the formation of cracks, typically near the MgAlCeMn phase. As shown in Fig. 5(a), the cracks were generated and developed near the needle-like MgAlCeMn phases. Such defects in the TRC experimental alloys are important because they led to the defects on the surface of experimental alloy strips during the solidification process (Fig. 5b). Fig. 5(c) shows that, with a UST power of 800 W, the needle-like MgAlCeMn phase was transformed to finer, globular particles. Although such MgAlCeMn particles were dispersed along the deformed roll casting direction, there were no microcracks around the globular-shaped intermetallics (Fig. 5c). This modification of the intermetallic MgAlCeMn by the UST improved the quality of the TRC magnesium alloy strips. As a result, the surface quality of the TRC Mg–Al–Zn–Ce–Mn alloy with a UST of 800 W improved significantly (Fig. 5d).

The microfeatures of the fracture surfaces of the Mg–Al–Zn–Ce–Mn alloy strips with or without UST after the tensile test are shown in Fig. 6. Both strips showed a hybrid ductile fracture with dimple and tear ridge, but micro-cracks could be observed near the intermetallics in the fracture surface. Therefore, modifying and refining the shape of the sharp edge intermetallic MgAlCeMn phase could improve the ductility and deformability of the TRC alloy strips.

4. Discussion

In this experiment, the fabricated TRC experimental alloy strips were approximately 3.6–4 mm in thickness. In many cases, during TRC processing, the microstructure of the TRC strip depended significantly on the solidification behavior of the liquid melt in the sump [19]. As the nucleation initiated from the roller surface, grains with the most favorable crystallographic orientation were able to grow and form the columnar dendrites [20]. Large columnar dendrites and coarse grains might result in problems during the solidification. Because the morphology of the dendrites was affected by the solidification process of the alloy, the introduction of powerful ultrasonic oscillations into the melt effectively alters the casting dendrites. The use of such ultrasonic oscillations could be simply adapted to a continuous TRC process. Therefore,

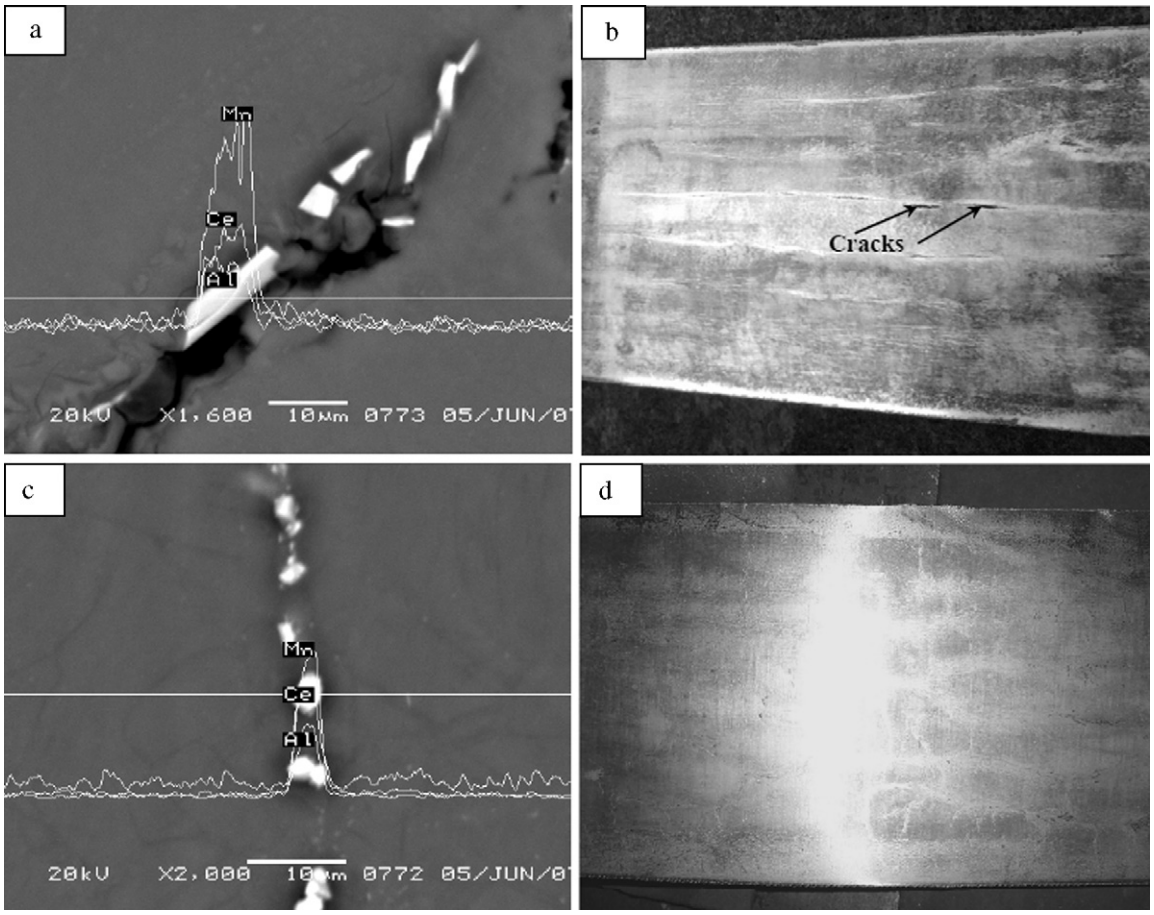

Fig. 5. Modification of ultrasonic treatment on the morphology of MgAlCeMn phase and the surface quality of twin roll casting experimental alloy: (a) needle-like-shaped MgAlCeMn phase and the cracks in the alloy without ultrasonic treatment; (b) surface cracks of the experimental alloy without ultrasonic treatment; (c) modified MgAlCeMn phase in experimental alloy with ultrasonic treatment and (d) good surface quality of experimental alloy with ultrasonic treatment.

we focused our discussion on the effects of UST on the grains and intermetallics formed in the TRC magnesium alloy used in this study.

4.1. Grain refinement mechanism of UST on TRC Mg–Al–Zn–Ce–Mn alloy

Generally, the ultrasonic treatment produced a "non-dendritic" structure, which consisted of globular grains without dendritic branching (Fig. 3d). The refined non-dendritic structure was advantageous because it led to a two-fold increase in plasticity with preserved strength. Comparing the tensile test results of the TRC experimental alloys with and without UST, the elongation of specimens treated with a UST power of 800 W increased from approximately 2% to 5% for the as-cast strip. Furthermore, the strength also increased with the improvement in elongation. The larger number of grain boundaries associated with finer α-Mg grains would clearly result in better mechanical properties. The relationship between the yield strength of the experimental alloy strips and the measured grain diameters are shown in Fig. 7.

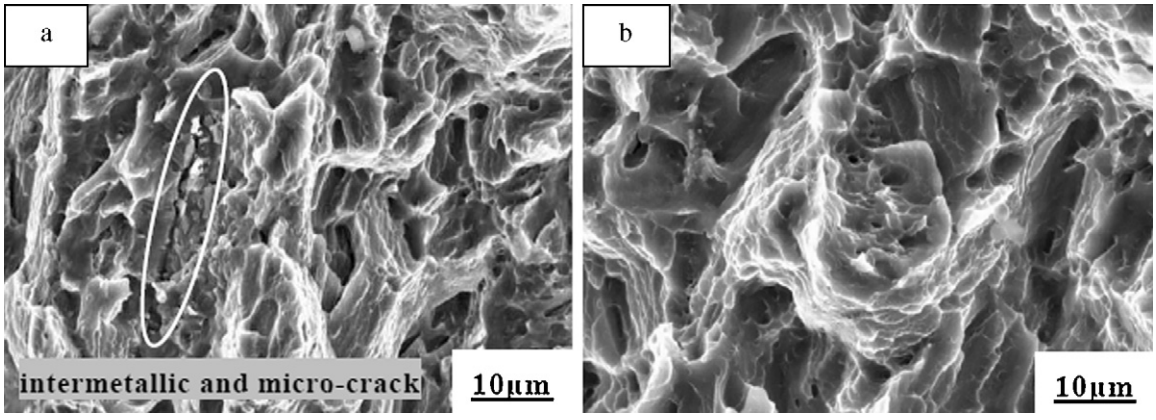

Fig. 6. Fracture surface of experimental alloy with and without ultrasonic treatment (a) fracture surface of experimental alloy without ultrasonic treatment and (b) fracture surface of experimental alloy with ultrasonic treatment.

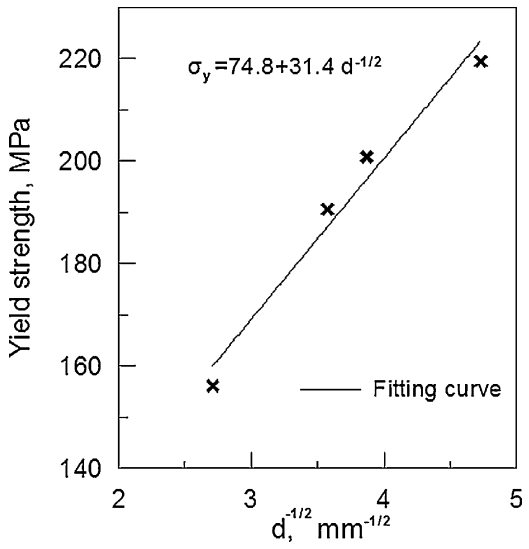

Fig. 7. Yield strength as a function of grain size ($d^{-1/2}$).

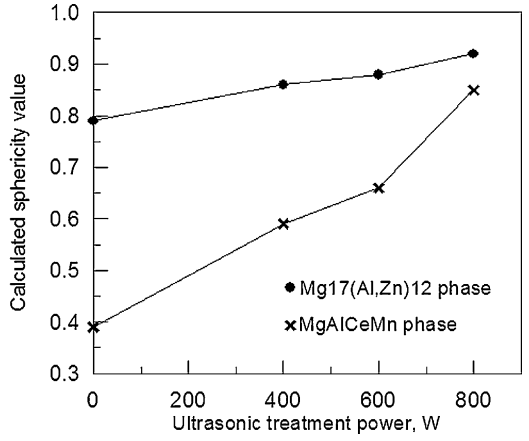

Fig. 8. Effects of ultrasonic treatment on the sphericity of intermetallics.

The curve fit of the experimental values demonstrated the linear relationship between these variables. These experimental results are in accordance with the well-known Hall–Petch equation. The relationship between the yield strength (σ_y) and the grain size (diameter, d) could be described as follows [21]:

$$\sigma_y = \frac{\sigma_0 + k}{(d)^{1/2}} \quad (1)$$

where σ_0 and k are constants related to the material. In this experiment, the relationship between the refined grain sizes created by UST and the yield strength of the TRC experimental strip could be written as follows:

$$\sigma_y = 74.8 + 31.4 \times d^{-1/2} \quad (2)$$

The increase in measured yield strength in the experiment was approximately 28%, which matched well with the calculated value. This result also matched the referenced parameters [22].

The development of acoustic cavitation in the UST created favorable conditions for heat and mass transfer processes during solidification. Cavitation refined the cast microstructure and removed the gases and oxides from the molten alloy [23]. During UST, the cavity was formed when the melt was subjected to random compression–expansion cycles. The cavity grew continuously until it collapsed and produced a high-intensity shock wave in the melt. The induced cavitation enabled radical changes in both grain nucleation and growth during solidification [24]. Two types of mechanisms may explain the cavitation-aided grain refinement. The first possible explanation is based on the principles of grain multiplication, and the second relies upon cavitation-induced heterogeneous nucleation. The grain multiplication theory is based on the idea that shock waves generated from the bubbles collapse. This shock wave leads to fragmentation of dendrites, and the fragments are then distributed by acoustic streaming within the whole melt volume, which ultimately increases the number of solidification sites. This mechanism of cavitation treatment requires the presence of growing dendrites. Such a mechanism may explain the phenomenon that occurred at the relative low ultrasonic powers of 400 W and 600 W in this experiment. The grain morphology included both dendrites and "non-dendritic" structures, and the dendrites may have provided the fragments needed as solidifying sites for "non-dendritic" structures.

When an ultrasonic power of 800 W was utilized in this investigation, almost no dendrite structures were generated. In this case, fragmentation of dendrites could not be the mechanism for grain multiplication. Cavitation-induced heterogeneous nucleation was further proposed to explain the refinement of grains. The ultrasonic vibrations were introduced in the molten experimental alloy liquid in the header-box and produced the acoustic cavitation to ensure the improvement the nucleation of α-Mg during the solidification process. On one hand, under the experimental conditions employed in this study, ultrasonic cavitation could clean the surfaces of poorly wetted particles in the melt and thereby enhance their nucleation potency. Even particles with large wetting angles were activated and contributed to nucleation, which resulted in a non-dendritic structure. On the other hand, with the UST applied to the melt, the local pressure in some parts of the molten experimental alloy liquid in the header box would increase to approximately 100–1000 MPa [25]. Such a phenomenon was produced by the cavitation of UST that generated local pressure pulses. Based on the Clausius–Clapeyron relation [26], the melting point would increase as the bubble collapses. The melting temperature of the local alloy would increase approximately 100–120 K under such pressure. This was equivalent to increasing the undercooling, which would promote heterogeneous nucleation in the melt. The refined equiaxed grains were obtained with high ultrasonic power.

4.2. Intermetallic modification mechanism of UST on TRC Mg–Al–Zn–Ce–Mn alloy

The modification efficiency of needle-like shaped intermetallics in the TRC Mg–Al–Zn–Ce–Mn alloy may be illustrated by calculating the sphericity values. The sphericity (Ψ) is a measure of how spherical (round) an object is. The sphericity of each particle is described as follows:

$$\Psi = \frac{\sqrt[3]{\pi(6V_P)^2}}{A_P} \quad (3)$$

where V_P is volume of the particle and A_P is the surface area of the particle. However, because the surface area must be evaluated by three-dimensional shape analysis, this ratio cannot be determined by the present two-dimensional measurement method. Therefore, an alternative definition of sphericity in two-dimensions is used. It is given by the following equality (4) [27]:

$$\Psi = \frac{4\pi A_P}{L^2} \quad (4)$$

where L is the perimeter of particle and A_P is the area of the particle.

With the metallographic analysis software, the areas and the perimeters of both $Mg_{17}(Al,Zn)_{12}$ and MgAlCeMn phases may be provided under different ultrasonic power conditions. The variation of calculated sphericity is shown in Fig. 8. Usually, as the

calculated sphericity value increases, the intermetallic becomes more globular. Because the morphology of the $Mg_{17}(Al,Zn)_{12}$ phase was initially observed to be round (Fig. 4), the sphericity increase of this phase was not as dramatic as that of the MgAlCeMn phase. As previously mentioned, the more globular MgAlCeMn intermetallic would increase the deformability of the TRC experimental alloy strips.

Although both the MgAlCeMn and the $Mg_{17}(Al,Zn)_{12}$ phases were refined or modified by the UST during solidification, different mechanisms may have been responsible for these changes due to the different formation temperatures of two intermetallic phases. The dominant $Mg_{17}(Al,Zn)_{12}$ phase formed by an eutectic reaction in the Mg–Al–Zn system at about 710 K [9]. Due to its low formation temperature, the $Mg_{17}(Al,Zn)_{12}$ phase was the last solid phase formed during solidification and distributed on the grain boundaries α-Mg. Therefore, the larger number of grain boundaries and the chemical composition gradients on the liquid/solid interface result in precipitation of this phase in more locations. In addition, the cavitation phenomenon produced by UST in the melt could clean the surfaces of the particles in the melt and improve the heterogeneous nucleation of the $Mg_{17}(Al,Zn)_{12}$ phase.

The MgAlCeMn phase formed in a peritectic reaction at temperatures exceeding 931 K. There was only alloy liquid, and no other phases, such as α-Mg or $Mg_{17}(Al,Zn)_{12}$, were expected to form at such high temperature. Therefore, there must be another mechanism responsible for the refinement and modification of the MgAlCeMn phase. The thermo-physical properties of molten magnesium and the previously described effect of the Clausius–Clapeyron relation result in a sudden local undercooling in the melt. These processes would improve nucleation of the MgAlCeMn phase. The gas in the bubbles produced by the cavitation of UST would rapidly expand at such high temperatures. This expansion would cause undercooling at the bubble surface and, as a result, nucleation of the MgAlCeMn phase. When these bubbles collapsed, they generated a significant number of nuclei for the MgAlCeMn phase. Because the UST was introduced in the melt in the header-box where the molten alloy flowed into the rollers for solidification, greater UST power led to better penetration of the melt, the addition of bubble production and greater undercooling. The intermetallic MgAlCeMn phase was significantly refined by the UST with the power of 800 W, and its needle-like morphology with sharp edges was transformed to a globular shape.

5. Conclusion

In summary, UST promoted grain refinement of α-Mg and modification of intermetallic $Mg_{17}(Al,Zn)_{12}$ and MgAlCeMn phases of the TRC Mg–3 wt%Al–1%Zn–0.8%Ce–0.3%Mn alloy. In this experiment, with the UST power of 800 W, the grain size of α-Mg decreased from 136.3 μm to 44.7 μm, and the morphology of α-Mg changed from dendritic to globular. The UST also modified the needle-like shaped intermetallic MgAlCeMn phase to a more globular phase with finer particles. A cavitation phenomenon was responsible for the effects of UST on the experimental magnesium alloy. Both grain multiplication by fragmentation of dendrites and cavitation-induced heterogeneous nucleation were proposed to explain the refinement of α-Mg grains by UST during TRC. Different mechanisms were proposed to explain the refinement or modification of the intermetallics due to their different characteristics. The larger number of grain boundaries and the particle-cleaned surface created by UST in the melt improved the heterogeneous nucleation of the $Mg_{17}(Al,Zn)_{12}$ phase. The modification of the MgAlCeMn phase was the result of the undercooling created by the cavitation of UST.

Improved microstructures contributed to the increase in both tensile strength and elongation of the TRC experimental magnesium alloy. The relationship between yield strength and the refined grain sizes of the experimental alloy subject to UST may be expressed with the Hall–Petch equation $\sigma_y = 74.8 + 31.4 \times d^{-1/2}$.

In this investigation, we explored the microstructure and properties of TRC Mg–3 wt%Al–1%Zn–0.8%Ce–0.3%Mn alloy strips and the effects of UST. Such research is important for the manufacturing of magnesium alloy sheets. Further studies of the subsequent rolling, heat treatment or plastic formation of TRC magnesium alloy sheets will be presented in another paper.

Acknowledgments

This work was supported by a Canada-China-USA Collaborative Research & Development Project, Magnesium Front End Research and Development (MFERD).

References

[1] B.L. Mordike, T. Ebert, Mater. Sci. Eng. A 302 (2001) 37–45.
[2] E. Mark, B. Aiden, B. Matthew, D. Chris, D. Gordon, D. Yvonne, JOM 60 (2008) 57–62.
[3] C.J. Bettles, M.A. Gibson, JOM 57 (2005) 46–49.
[4] R. Kawalla, M. Oswald, C. Schmidt, M. Ullmann, H.P. Vogp, N.D. Cuong, Metalurgua 47 (2008) 195–198.
[5] http://www.transportation.anl.gov/pdfs/TA/101.pdf.
[6] S.S. Park, W.J. Park, C.H. Kim, B.S. You, JOM 61 (2009) 14–18.
[7] H. Watari, T. Haga, N. Koga, K. Davey, J. Mater. Proc. Tech. 192–193 (2007) 300–305.
[8] H. Watari, K. Davey, M.T. Rasgado, T. Haga, S. Izawa, J. Mater. Proc. Tech. 155–156 (2004) 1662–1667.
[9] A.A. Kaya, O. Duygulu, S. Ucuncuoglu, G. Oktay, D.S. Temur, O. Yucel, Trans. Nonferrous Met. Soc. China 18 (2008) 185–188.
[10] Z. Bian, I. Bayandorian, H.W. Zhang, G. Scamans, Z. Fan, Mater. Sci. Tech. 25 (2009) 599–605.
[11] S.X. Song, J.A. Horton, N.J. Kim, T.G. Nieh, Scripta Mater. 56 (2007) 393–395.
[12] G. Song, A.L. Bowles, D.H. St. John, Mater. Sci. Eng. A 366 (2004) 472–476.
[13] A. Wu, C.Q. Xia, S. Wang, Rare Met. 25 (2006) 371–376.
[14] L.L. Rokhlin, Magnesium Alloys Containing Rare Earth Metals: Structure And Properties, Taylor & Francis, London, 2003.
[15] K. Yu, W.X. Li, J. Zhao, Z. Ma, R. Wang, Scripta Mater. 48 (2003) 1319–1322.
[16] T.V. Atamanenko, D.G. Eskin, L. Zhang, L. Katgerman, Metall. Mater. Trans. A 41A (2010) 2056–2066.
[17] A. Ramirez, M. Qian, B. Davis, T. Wilks, D.H. StJohn, Scripta Mater. 59 (2008) 19–22.
[18] G.I. Eskin, Adv. Perform. Mater. 4 (1997) 223–232.
[19] T. Haga, H. Watari, S. Kumai, J. Achiev. Mater. & Manuf. Eng. 15 (2006) 186–192.
[20] Z. Bian, I. Bayandorian, H.W. Zhang, Z. Fan, Solid State Phenom. 141–143 (2008) 195–200.
[21] W.F. Smith, J. Hashemi, Foundations of Materials Science and Engineering, fifth ed., Mc Graw Hill, New York, 2010.
[22] N. Ono, R. Nowak, S. Miura, Mater. Lett. 58 (2003) 39–43.
[23] M. Qian, A. Ramirez, A. Das, D.H. StJohn, J. Cryst. Growth 312 (2010) 2267–2272.
[24] G.I. Eskin, Ultrason. Sonochem. 8 (2001) 319–325.
[25] M.K. Aghayani, B. Niroumand, J. Alloys Compd. 509 (2011) 114–122.
[26] http://en.wikipedia.org/wiki/Clausius%E2%80%93Clapeyron_relation.
[27] http://en.wikipedia.org/wiki/Sphericity.